American Mineralogist, Volume 83, pages 1516–1531, 1998

Effects of microbial activity on the $\delta^{18}O$ of dissolved inorganic phosphate and textural features of synthetic apatites

R.E. BLAKE,[1,*] J.R. O'NEIL,[1] AND G.A. GARCIA[2]

[1]Department of Geological Sciences, University of Michigan, Ann Arbor, Michigan 48109-1063, U.S.A.
[2]Interdepartmental Program in Medicinal Chemistry, University of Michigan, Ann Arbor, Michigan 48109-1065, U.S.A.

ABSTRACT

Laboratory growth experiments were conducted to investigate the oxygen isotope effects associated with bacterial metabolism of phosphatic compounds commonly available in nature. The observed oxygen isotope fractionations suggest complex patterns of exchange between dissolved inorganic phosphate (P_i) and water, and significant circulation of P_i between intracellular and extracellular locations with extensive recycling of the dissolved P_i pool, even at high concentrations of dissolved P_i. Results of these experiments also support current models for bacterial utilization of phosphate. These results have important implications for the use of $\delta^{18}O$ values of dissolved P_i to trace sources of P, and bear on integrity of original oxygen isotope compositions of biogenic and sedimentary apatite minerals that have been subjected to processes of recrystallization and diagenesis.

SEM images of laboratory synthesized apatite minerals show that similar textural features may be produced by microbially mediated and abiotic reactions, and that spheroidal structures may be produced by processes of dissolution as well as precipitation. The interpretation of certain mineral structures as microbial in origin solely on the basis of morphological and textural features may be misleading.

INTRODUCTION

Geologists have long recognized the ubiquitous presence of bacteria in sediments, aquifers, and pore water environments, but the effects of microbially mediated reactions on geochemical processes and specific interactions between bacteria and mineral surfaces have only recently received widespread attention. Bacteria are important in the geochemical cycles of elements such as P, N, and S. Microbial metabolic activity may completely dominate pore water chemistry, for example, in shallow marine sediments where bacterial sulfate reduction is highly pronounced. Bacteria have also been implicated as important mediators of both the dissolution and precipitation of various minerals including carbonates (Buczynski and Chafetz 1991; Folk 1993; Jones 1995; Vasconcelos and McKenzie 1997), silicates (Ullman et al. 1996; Bennett et al. 1996; Folk and Lynch 1997), metal oxides (Lovely et al. 1987; Mandernack et al. 1995; Grantham and Dove 1996; Brown et al. 1997), phosphates (O'Brien et al. 1981; Lucas and Prevot 1984; Hirschler et al. 1990), and phosphorite deposits (e.g., Prevot and Lucas 1986; Soudry 1987; Rao and Nair 1988; Soudry and Southgate 1989; Lamboy 1990; Bertrand-Sarfati et al. 1997). Microorganisms are especially important in the cycling of phosphorus in aquatic and sedimentary environments (Chrost 1991; Goldstein 1994). Degradation of organic matter by bacterial enzymes provides a major source of dissolved inorganic phosphate (P_i) to the water column and to pore fluids where it is consumed as a preferred nutrient by microorganisms and plants (Ammerman 1991), and may be precipitated as authigenic apatite minerals (Prevot and Lucas 1986; Hirschler et al. 1990, 1992).

Oxygen isotope ratios of phosphates and biogenic apatites are used in paleoclimatological and environmental studies to obtain critical information on temperatures of formation and environmental conditions under which phosphate minerals are formed (e.g., Ayliffe and Chivas 1990; D'Angela and Longinelli 1993; Barrick and Showers 1994; Fricke et al. 1996; Kohn et al. 1996), and also to identify sources of dissolved phosphate in aquatic ecosystems (Markel et al. 1994; Gruau et al. 1997). Correct interpretation of oxygen isotope ratios in phosphates thus requires understanding all processes and reactions leading to alteration of primary isotopic compositions or fractionation of oxygen isotopes, and the factors that govern these processes. Very few investigations have been made of the oxygen isotope effects associated with microbial metabolism of phosphate (e.g., Paytan 1989; Blake et al. 1997).

Oxygen isotope systematics of phosphate in more complex organisms such as mammals, fish, and marine invertebrates, indicate that phosphate ingested by these organisms undergoes complete isotopic exchange with internal body fluids and is precipitated (e.g., as bone or

* Current address: Yale University, Geology and Geophysics, New Haven, Connecticut 06511, U.S.A. E-mail: blake@hess.geology.yale.edu.

0003–004X/98/1112–1516$05.00

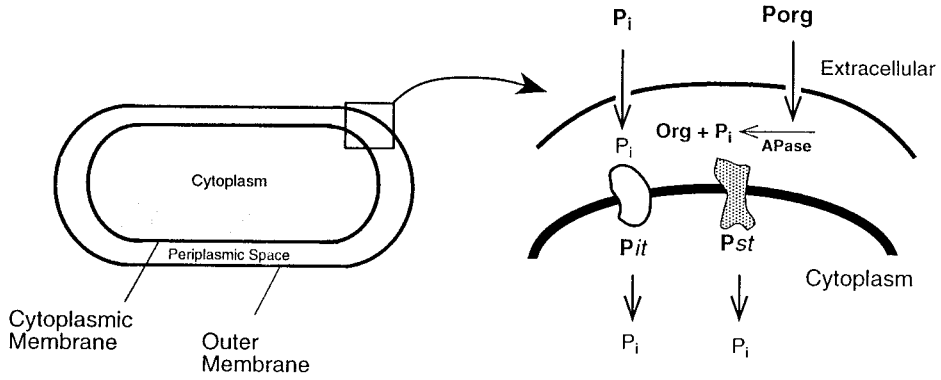

FIGURE 1. Schematic illustration of bacterial membrane structure. The two major phosphate transport systems in bacteria are: P*it* (inorganic phosphate transport) and P*st* (phosphate specific transport). Inorganic (P_i) and organically bound P (P_{org}), are taken up first through pores in the outer membrane. The P*it* system operates under conditions of plentiful P_i availability. The P*st* P_i transport system is induced by conditions of P_i limitation. The P*st* system operates in conjunction with phosphate-scavenging enzymes such as alkaline phosphatase (APase) that catalyze the release of organically bound P_i to the medium. This P_i is subsequently taken up by cells through the P*st* transport system.

tooth) in oxygen isotope equilibrium with body water (Kolodny et al. 1983; Luz and Kolodny 1985; Longinelli 1993; Lecuyer et al. 1996). Unlike ''higher'' organisms, bacteria cannot readily ingest or take up complex organic molecules that are commonly a primary source of available P in nature. Instead, bacteria must break down and release P_i from these molecules via enzyme-catalyzed reactions occurring outside of the cytoplasm of the cell, under the relatively open-system conditions of the extracellular medium or periplasmic space (Fig. 1). These enzymatic hydrolysis reactions involve the incorporation of water into P_i that is released to the medium. The specific oxygen isotope exchange properties (e.g., equilibrium exchange, partial exchange) associated with these important reactions of phosphate, however, are not well known. In light of the important role of microbial activity in geochemical cycling of phosphate and formation of authigenic apatite and sedimentary phosphate minerals, these conditions point to the critical need for thorough characterization of the oxygen isotope effects associated with bacterial metabolism of various phosphatic compounds encountered in nature.

In an earlier paper (Blake et al. 1997), we reported results of bacterial culture experiments that demonstrated significant, but incomplete exchange of oxygen isotopes between phosphate liberated during microbial metabolism of nucleic acid (RNA) and water. Nucleic acids are phosphodiesters representative of complex organophosphate (P_{org}) compounds found in nature (Fig. 2). The observed isotopic fractionations were reproducible and were apparently governed by equilibrium isotope effects. In the case of RNA, the extent of phosphate-water exchange appeared to be related to the internal bonding and molecular configuration of the P_{org} compound. In initial bacterial growth experiments using dissolved P_i as the source of phosphorus for growth, extensive exchange of oxygen isotopes between P_i and water was also demonstrated.

Here we present results of new experiments that probe further the mechanisms and patterns of isotopic exchange between dissolved phosphate and water during bacterial metabolism of specific types of phosphatic compounds. The isotopic exchange accompanying bacterial metabolism of P_i is of special interest here, due to the potential impact of such exchange on the oxygen isotope ratios of phosphate ($\delta^{18}O_p$) in authigenic or recrystallized sedimentary and biogenic apatites that are used to reconstruct paleoenvironmental conditions. Textural features observed in laboratory synthesized apatites are also presented and discussed in the context of proposed mechanisms of phosphatogenesis.

MATERIALS AND METHODS

Bacterial culture and growth

Bacteria were grown on defined minimal media containing either inorganic orthophosphate or organically bound phosphate as a sole source of phosphorus. Phosphatic compounds having different molecular configurations and different metabolic pathways were chosen to investigate the relations between isotopic fractionation patterns, the molecular configuration, and the metabolic pathway utilized by the organism. Growth media were prepared with waters having a wide range of oxygen isotope compositions to identify the extent of PO_4-water isotopic exchange. All experiments were conducted under sterile conditions in pure culture. Experiments were carried out between 5.7 and 35 °C in temperature-controlled environmental chambers or water baths.

The bacterium *Klebsiella aerogenes* was grown on a minimal salts medium containing glucose-1-phosphate as a sole source of phosphorus and carbon. The glucose-1-phosphate medium comprised 6 g/L glucose-1-phosphate, 2.4 g/L NH_4Cl, 1.6 g/L $CaCO_3$, 0.13 g/L NaF, and 4.0 g/L HEPES (N-[2-Hydroxyethyl] piperizine-N′-[2-ethane-

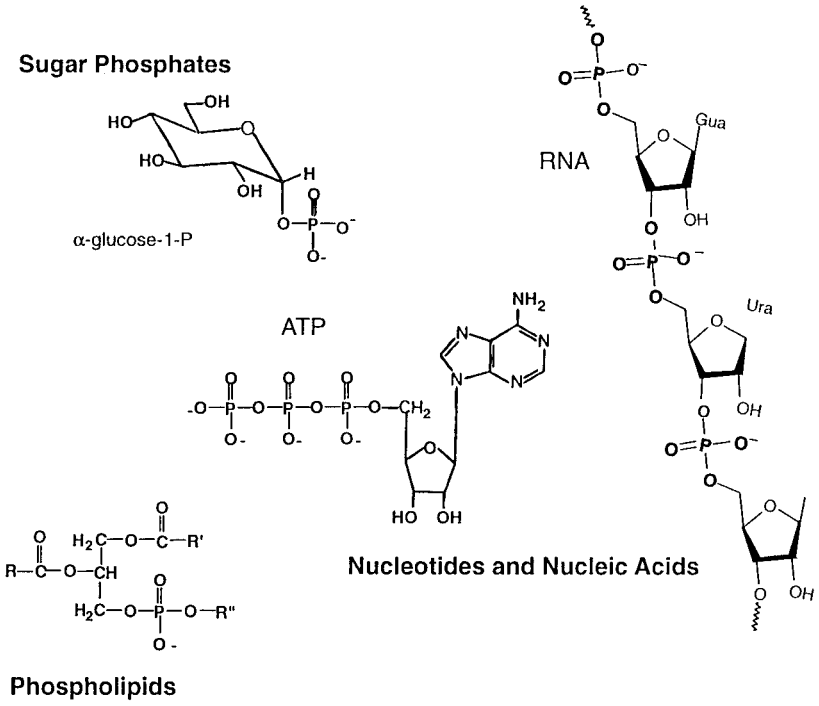

FIGURE 2. Representative forms of organically bound phosphate commonly encountered in nature. Note phosphodiester backbone in RNA.

sulfonic acid]) and was adjusted to pH 7 with 1 N NaOH. These experiments were inoculated with equivalent amounts of *K. aerogenes* (≤48 h old) suspended in a pH 7 buffer solution. Sodium fluoride and $CaCO_3$ were added to promote the precipitation of P_i released from glucose-1-phosphate as fluorapatite following the methods of Lucas and Prevot (1984). P_i was extracted from the media as fluorapatite as described in Blake et al. (1997). The $\delta^{18}O_w$ values of the growth media were −18.2, −6.7, and 42.2‰. These experiments were carried out in Nephelotype flasks at 25 °C in a reciprocal shaking water bath at 90 r.p.m. Cell densities and growth rates were determined by measuring the absorbance at 660 nm (A_{660}). The amount of dissolved P_i released to the growth medium was determined as a function of time from periodic aseptic extractions of growth medium.

The growth medium used in experiments on inorganic phosphate (5 m*M* P_i as KH_2PO_4) metabolism contained 0.6% glucose, 0.68 g/L KH_2PO_4, 1.87 g/l NH_4Cl, and 0.1 g/L $MgSO_4$ with 50 m*M* TRIS [Tris (hydroxymethyl) aminomethane-HCl] buffer; the pH was adjusted to 7 using NaOH. The oxygen isotope compositions of waters ($\delta^{18}O_w$) used to prepare the media ranged from −18.8 to 99.0‰. Experiments were carried out in bioreactor vessels that were specifically designed to provide aeration/agitation while maintaining constant $\delta^{18}O_w$ values of the growth media (Blake et al. 1997). The growth temperatures investigated were 5.7, 10.0, 15.1, 25.0, and 35.0 ± 0.1 °C. This wide range of temperatures required the use of different strains of bacteria that could grow optimally at the given temperatures. Cold-tolerant strains obtained from the American Type Culture Collection (ATCC) were used in experiments at temperatures below 20 °C. *Aquaspirillum arcticum* (ATCC no. 49402), *Psychrobacter immobilis* (ATCC no. 15174), and *Bacillus psychrophilus* (ATCC no. 23305) strains with optimum growth temperatures of 4, 10, and 15 °C, respectively, were used in experiments at 5.7, 10.0, and 15.1 °C. A *Klebsiella aerogenes s*train kindly supplied by R. Bender of the University of Michigan, was used in the 5 m*M* P_i experiments at 25 and 35 °C. The pure strains were stored frozen in glycerol-water (1:1 weight proportions) at liquid nitrogen temperature. An earlier series of experiments, described previously in Blake et al. (1997) and reported here for comparison, was carried out in 10 m*M* P_i growth media at 25 °C using mixed cultures of bacteria isolated from freshwater ponds and soils.

Experimental growth media were inoculated using bacterial colonies (≤48 h old) that were suspended in 50 m*M* TRIS buffer to a uniform cell density and then pipetted into the reaction vessels in equal amounts. Cultures were incubated for periods of 30–68 days. Dissolved P_i was isolated from 5 m*M* P_i experimental solutions for isotopic analysis by quantitative precipitation as ammonium phosphomolybdate (APM), after solutions had been centrifuged to remove bacterial cells as a cell pellet. The APM precipitate was then recrystallized as magnesium ammonium phosphate (MAP) and finally as silver phosphate, the compound used for determination of $\delta^{18}O_p$.

In experiments where microbially processed phosphate was precipitated as fluorapatite, the solids were routinely examined under SEM to study various textural features produced during microbially mediated apatite synthesis. Several examples of the textural features observed in lab-

TABLE 1. Oxygen isotope compositions of synthetic fluorapatite and fluids

$\delta^{18}O_w$	$\delta^{18}O_p$ Observed	$\delta^{18}O_p$ at equil.*	Theoretical inherited $\delta^{18}O_p$†
−18.2	6.5	1.9	−24.9
−6.7	14.1	13.4	−13.7
42.2	53.3	62.3	35.5

Note: From glucose-1-phosphate experiments at 25 °C with *K. aerogenes*. All $\delta^{18}O$ values are ± 0.1‰.

* Equilibrium $\delta^{18}O_p$ values based on equation of Longinelli and Nuti (1973).

† Calculated using Equation 2.

oratory synthesized apatites are presented and the implications of these features for interpretation of the origin of sedimentary phosphate deposits are discussed.

Analytical methods

Apatites were converted to Ag_3PO_4 for oxygen isotope analyses using the method of O'Neil et al. (1994). The analytical precision of this method is ±0.2‰ (1σ) or better. Oxygen isotope ratios of fluids were determined using the CO_2-H_2O equilibration method (Cohn and Urey 1938) with analytical precision of better than ±0.1‰ (1σ). Isotopic analyses were performed at the University of Michigan in the Stable Isotope Laboratory (ISOLAB) on a Finnigan Mat Delta S stable isotope ratio mass spectrometer and are reported using the standard delta (δ) notation in per mil (‰) relative to the SMOW international reference standard. The fractionation factor, α, between phosphate (p) and water (w) is defined here as:

$$\alpha_{p-w} = (1 + \delta^{18}O_p/1000)/(1 + \delta^{18}O_w/1000). \quad (1)$$

SEM analyses were performed using a Hitachi Model S-570 scanning electron microscope fitted with backscattered and secondary electron detectors, and a Kevex quantum energy dispersive X-ray analytical system at the University of Michigan (EMAL) facility. All other chemical analyses were made in the University of Michigan Experimental and Analytical Geochemistry Laboratory (EAGL). Dissolved P_i was determined colorimetrically using the phosphomolybdate blue method (Koroleff 1983).

RESULTS AND DISCUSSION

Results of bacterial growth experiments and $\delta^{18}O$ values of phosphate and fluids are presented in Tables 1 and 2. The $\delta^{18}O_p$ values measured in most experiments demonstrate significant exchange of oxygen isotopes between dissolved phosphate and water during bacterial metabolism of both dissolved inorganic phosphate (P_i medium) and glucose-1-phosphate.

Experiments with glucose-1-phosphate

As stated above, phosphorus is often available to microorganisms primarily in the form of organic matter, which first must be broken down and dephosphorylated outside of the cell (Fig. 1). Phosphomonoesters and phosphodiesters are the most common forms of organophosphorus compounds encountered in natural systems (Fig. 2; Paul and Clark 1989; Ingall et al. 1990). Glucose-1-phosphate was used here as a representative phosphomonoester compound. It has been demonstrated that glucose-1-phosphate must be dephosphorylated extracellularly prior to uptake of glucose or P_i by bacterial cells (Kadner et al. 1994). Growth rates of the bacterium *K. aerogenes* were very similar in glucose-1-phosphate media prepared using three isotopically distinct waters (Fig. 3a). The release of free P_i to the medium via bacterial degradation of this phosphomonoester substrate also followed a similar course in the three experiments (Fig. 3b). When bacteria are grown under conditions of P_i deprivation, as in these experiments using organically bound phosphate as the sole P_i source, the production of enzymes capable of releasing organically bound P_i is increased greatly. The time required for synthesis of these so-called ''phosphate-scavenging'' enzymes is evidenced by an initial lag in growth as seen in the early region of the growth curve in Figure 3a. This initial lag period is followed by exponential growth of bacterial cells and a concomitant release of P_i to the growth medium.

In previous experiments, where bacteria were grown on a phosphodiester (RNA, a nucleic acid), the observed amount of oxygen isotope exchange was found to be related to the number of phosphoester bond linkages (P-O-

TABLE 2. Oxygen isotope compositions of dissolved phosphate and fluids

Extraction time (days)	*T* (°C)	$\delta^{18}O_w$	$\delta^{18}O_p$	Expected $\delta^{18}O_p$ at equil.*
		5 m*M* P_i media		
50	5.7	−8.2	14.4	16.4
68	10†	−8.2	14.3	15.4
32	15‡	−8.2	15.0	14.2
7	35§	−8.2	15.3	9.6
38	35	−8.2	14.6	9.6
26	5.7	−18.8	14.0	5.8
32	10	−18.8	14.3	4.8
32	15	−18.8	13.4	3.6
68	15	−18.8	12.3	3.6
68	25§	−18.8	10.7	1.3
68	35	−18.8	12.3	−1.0
50	5.7	99.0	15.7	123.6
32	10	99.0	17.5	122.6
32	15	99.0	43.3	121.4
68	25	99.0	74.8	119.1
7	35	99.0	28.8	116.8
		10 m*M* P_i media		
68	25	−17.7	9.3	2.4
68	25	−6.0	18.6	14.1
68	25	12.6	33.9	32.7

Note: From P_i media experiments. Initial KH_2PO_4 $\delta^{18}O_p$ = 13.5‰. $\delta^{18}O_w$ values changed by <0.3‰ over course of experiments. All $\delta^{18}O_p$ values are ± 0.3‰.

* Equilibrium $\delta^{18}O_p$ values based on equation of Longinelli and Nuti (1973).

† Inoculated with *P. immobilus*; optimum growth at 10 °C.

‡ Inoculated with *B. psychrophilus*; optimum growth at 15 °C.

§ Inoculated with *K. aerogenes*; optimum growth 30 °C.

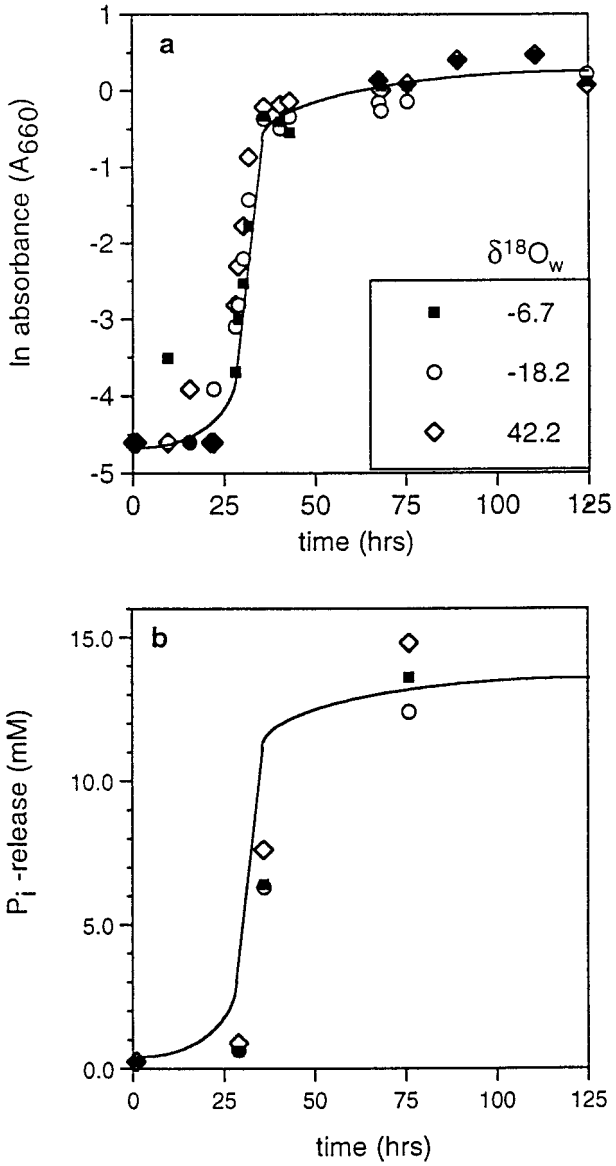

FIGURE 3. (**a**) Growth curves for *K. aerogenes* at 25 °C on glucose-1-phosphate medium: 6 g/L glucose -1-phosphate; 2.4 g/L NH_4Cl; 1.6 g/L $CaCO_3$; 0.13g/L NaF; 4.0g/L HEPES; adjusted to pH 7.0 with 1N NaOH. Cell density determined by absorbance at 660 nm (A_{660}). Note similar growth rates for all three cultures. (**b**) Dissolved inorganic phosphate (P_i) released to growth medium as a function of time.

C) present in the substrate (Blake et al. 1997). According to this model, a phosphodiester such as RNA, which has two phosphoester linkages and thus requires lysis of at least two extracellular P-O bond, to release free P_i to the medium, will exhibit exchange of oxygen with water at the 2 sites of bond hydrolysis (i.e., at two of the four O atoms in PO_4), with the remaining two O atoms being inherited from the original phosphodiester substrate (Fig. 4a). In the case of RNA, the exchange of oxygen between P_i and water appeared to be governed by equilibrium isotope effects. Evidence in support of this model is provided by the results of Bruice et al. (1995). In experiments on the chemical (non-enzymatic) hydrolysis of phenylphosphodiester compounds using ^{18}O-labeled compounds (50% ^{18}O) to probe the reaction mechanism, these researchers demonstrated the incorporation of ^{18}O at only 2 sites (i.e., 50% of sites) in the final orthophosphate product released to solution.

It follows from the results of RNA experiments that P_i released from a phosphomonoester such as glucose-1-phosphate, which has only one phosphoester linkage, will exchange with water at only one oxygen site in PO_4. This reaction is most likely catalyzed by a phosphomonoesterase enzyme such as alkaline phosphatase (Fig. 4b). Thus, we can predict that 25% of the oxygen in P_i released from glucose-1-phosphate will reflect equilibrium isotope exchange with water whereas the remaining 75% will be inherited from the original substrate. An important assumption made in using this approach is that the enzyme-catalyzed hydrolysis of P-O bonds in glucose-1-phosphate also will be accompanied by equilibrium isotope effects, as was observed for the hydrolysis of P-O bonds in RNA (Blake et al. 1997).

Dissolved P_i precipitated from glucose-1-phosphate growth experiments, which had $\delta^{18}O_w$ values of −18.2, −6.7, and 42.2‰, had $\delta^{18}O_p$ values of 6.5, 14.1, and 53.3‰, respectively (Table 1). At 25 °C, the equilibrium fractionation between apatite and water, using the Longinelli and Nuti (1973) equation, is 20.1‰, and the expected *equilibrium* $\delta^{18}O_p$ values are 1.9, 13.4, and 62.3‰, respectively. We assume here and throughout this manuscript that there is no oxygen isotope fractionation between dissolved phosphate and apatite. Incorporation of oxygen from water is clearly indicated by these $\delta^{18}O_p$ values, but the exchange reactions appear not to have reached equilibrium in all cases. Simple mixing equations of the form:

$$0.75x + 0.25\ (\delta^{18}O_p)_{eq} = (\delta^{18}O_p)_{obs} \qquad (2)$$

where x is the $\delta^{18}O$ value of oxygen inherited from glucose-1-phosphate, $(\delta^{18}O_p)_{eq}$ is the $\delta^{18}O_p$ value of apatite expected at equilibrium with water based on the Longinelli and Nuti (1973) relation, and $(\delta^{18}O_p)_{obs}$ is the observed value, show that 75% inheritance of some unique $\delta^{18}O_p$ component probably does not occur (Table 1). One explanation for this result is that the enzyme reaction catalyzing release of P_i from glucose-1-phosphate is not governed by equilibrium effects, as appeared to be the case with RNA (Blake et al. 1997). Alternatively, the P_i released from the initial extracellular enzymatic hydrolysis of glucose-1-phosphate may have been further exchanged with water during subsequent metabolic reactions catalyzed by the bacteria. This latter scenario is considered in much greater detail in the sections that follow.

If it is assumed that $\delta^{18}O_p$ values were shifting toward equilibrium values indicated by fractionation factors for phosphate and water (Table 1; Longinelli and Nuti 1973), then it appears that, in some experiments, much of the

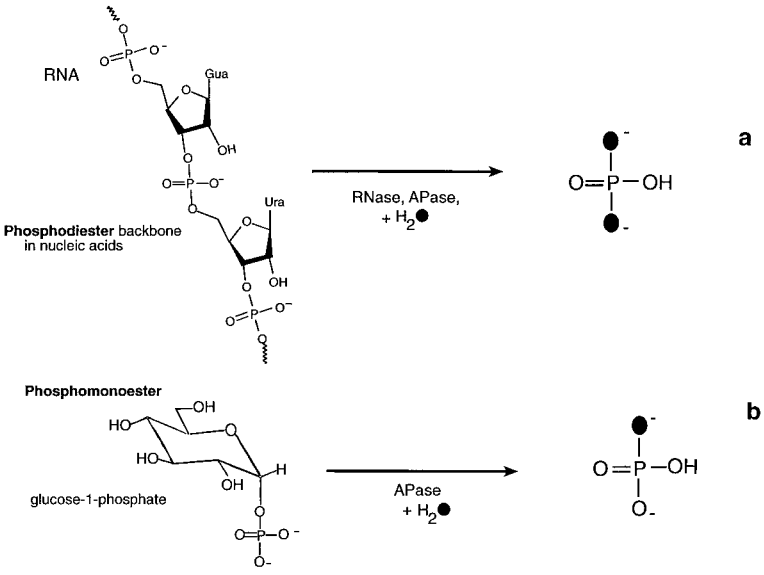

FIGURE 4. Incorporation of oxygen from water into P_i accompanying hydrolysis (i.e., attack by water) of P-O bonds in phosphoesters. (**a**) Phosphodiesters such as RNA require breaking of at least two P-O bonds to release "free" P_i, and thus, may incorporate oxygen from water at two sites in P_i. These bond-breaking reactions may be catalyzed by ribonuclease (RNase), a phosphodiesterase, followed by a phosphomonoesterase such as alkaline phosphatase (APase). (**b**) Phosphomonoesters require hydrolysis at only one P-O bond site to release P_i to the medium. This reaction is catalyzed by a phosphomonoesterase enzyme such as APase.

dissolved P_i pool underwent complete oxygen isotope exchange and equilibration with water. $\delta^{18}O_p$ values obtained in experiments using water with more negative $\delta^{18}O_w$ values (−18.2‰) are more positive than expected, whereas apatite precipitated from the medium with a very positive $\delta^{18}O_w$ value (42.2‰) is more negative than expected (Table 1). This pattern suggests the contribution of oxygen from a source or process that generates oxygen having an intermediate $\delta^{18}O$ value. Similar patterns were observed in experiments using RNA and waters with different $\delta^{18}O$ values (Blake et al. 1997). It is difficult to interpret mixing relationships and possible contributions from different oxygen sources further without knowledge of the specific reaction mechanisms catalyzing the isotopic exchange and the isotopic effects (equilibrium vs. kinetic) associated with these mechanisms. Thus, results from experiments with glucose-1-phosphate may not confirm, but cannot rule out, the 50% inheritance model described for phosphodiesters. Unlike the experiments with RNA, which showed consistent patterns of P_i-water exchange, the metabolism of glucose-1-phosphate is characterized by more complex processes of oxygen isotope exchange and P_i turnover catalyzed by bacteria. More experimental data are needed to interpret the oxygen isotope fractionations observed in these experiments. Nonetheless, it is clear that the metabolism of glucose-1-phosphate by bacteria is accompanied by extensive exchange of oxygen isotopes between dissolved P_i and water.

P_i growth experiments

Inorganic phosphate growth experiments were conducted in waters having different oxygen isotope compositions over a temperature range of 5.7–35 °C to observe P_i-water oxygen isotope exchange patterns and to investigate the temperature dependence of these phosphate-water fractionations. As shown in Table 2, no appreciable change in $\delta^{18}O_p$ values was observed in some of the 5 m*M* P_i media experiments conducted at lower temperatures, even after periods of over 1 month. This observation may at first appear to indicate a lack of growth or extremely slow turnover of P_i in these experiments, but increased turbidity, development of characteristic filamentous forms in the case of *Aquaspirilum arcticum*, and other usual signs of growth were observed. As mentioned in the section on Materials and Methods, the wide range of temperatures used in these experiments required the use of different strains of bacteria that could grow at the given temperatures. The growth rates of bacteria may also vary with other conditions of growth such as the source of C and N. In general, cold-tolerant and psychrophilic bacteria grow more slowly than do mesophilic bacteria (growth optimum ~20–45 °C), even under optimum growth conditions, due to slower reaction rates at low temperature.

Another explanation for the apparent lack of turnover of dissolved P_i in some experiments may be that these particular strains of bacteria took up only small amounts of P_i from the medium, due to slow growth rates, and either converted it to organically bound biomass or stored it, for example, as polyphosphate (Kulaev 1994), instead of releasing it back into the medium. Increasing extent of exchange of oxygen isotopes between phosphate and water with increasing temperature was observed and is best illustrated in experiments with $\delta^{18}O_w$ = 99.0‰ between 5.7 and 25 °C (Table 2).

The possible mechanisms responsible for the patterns of isotopic fractionations and phosphate-water exchange observed in these experiments are considered further below in the context of proposed models of phosphate utilization by bacteria.

Oxygen isotope effects of P_i metabolism

Dissolved P_i is the preferred form of phosphate for bacterial growth. Unlike complex organophosphate com-

pounds, from which P_i must first be released by extracellular hydrolytic enzymes, dissolved P_i is readily taken up intact by most bacteria through specialized pores and transport proteins located in the cytoplasmic membrane (Fig. 1). This process does not require the action of hydrolytic enzymes or breaking of P-O bonds, and therefore should not be accompanied by exchange or fractionation of oxygen isotopes between P_i and water. Once inside the cytoplasm, P_i may be involved in numerous intracellular enzyme-catalyzed reactions that do involve the breakage and reformation of P-O bonds and that also, presumably, catalyze extensive oxygen isotope exchange between P_i and the intracellular water. Bacterial cytoplasmic membranes (Fig. 1) are impermeable to most molecules, but allow water to pass through them. Thus, similar to other aquatic organisms such as fish, the $\delta^{18}O_w$ of intracellular and extracellular fluids should be identical.

Bacterial cells maintain constant and relatively high levels of intracellular dissolved P_i (~10–30 m*M*), regardless of the growth conditions, concentrations, and types of P sources in the growth medium (Rosenberg et al. 1982; Rao et al. 1994). This intracellular P_i pool is very dynamic due to the rapid rates of P turnover within cells. Although bacteria readily take up dissolved P_i from the medium, mechanisms for release of this intracellular P_i, which presumably has been exchanged with water via intracellular enzyme reactions, can be very complex and depend upon the conditions of growth. Intracellular P_i is released from bacterial cells upon death and lysis, but the size of the collective bacterial intracellular P_i pools (i.e., from all of the cells) is so small compared to that of the extracellular dissolved P_i pool (<0.1% of extracellular P_i pool; Neidhardt 1987), that even release of intracellular P_i from all of the cells would not significantly impact the $\delta^{18}O_p$ value of dissolved P_i in the medium at a given point in time. Thus, in order for bacterial processes to produce significant shifts in the $\delta^{18}O_p$ values of the relatively large pools of dissolved P_i used in the P_i growth media (5–10 m*M*), the cells would have to take up P_i from the medium, turn it over and exchange/equilibrate the P_i with water during intracellular reactions, and then release P_i back into the medium. This process would have to be repeated many times to exchange/equilibrate the entire extracellular dissolved P_i pool with water. Release of intracellular P_i from bacterial cells and even circulation of P_i between intracellular and extracellular pools has been demonstrated for certain conditions of microbial growth (Rosenberg et al. 1982; Maloney 1992). However, the extent of these processes and their impact on oxygen isotope compositions of dissolved P_i in the medium was not known.

If we assume that all exchange of oxygen isotopes between P_i and water in the P_i media experiments is catalyzed within the cytoplasm of bacterial cells and that this exchange produces isotopic equilibrium between P_i and water, then the extent of turnover of P_i in the medium (i.e., circulation of this P_i between intracellular and extracellular regions) can be estimated by tracking the approach of $\delta^{18}O_p$ values of dissolved P_i toward expected equilibrium values. Over the course of the growth experiments, the percentage of dissolved P_i exchanged/equilibrated with water should increase from zero, for unmetabolized P_i at the start of the experiment, to 100% for turnover of the entire dissolved P_i pool.

$\delta^{18}O_p$ values of dissolved P_i in experiments conducted in solutions with $\delta^{18}O_w = -8.2$‰ and in the lower temperature experiments (<25 °C), changed least from the original starting value of 13.5‰ (Table 2). By contrast, experiments conducted in water with $\delta^{18}O_w = 99.0$‰ show clear evidence of P_i-water exchange and phosphate turnover, even at 10 and 15 °C. $\delta^{18}O_p$ values expected for equilibrium oxygen isotope exchange (Table 2) indicate that, in experiments with $\delta^{18}O_w = -8.2$‰, the initial KH_2PO_4 ($\delta^{18}O_p = 13.5$‰) was already close to equilibrium with this water. The $\delta^{18}O_p$ values, therefore, did not need to change much to reach equilibrium. Larger shifts in $\delta^{18}O_p$ values were observed in experiments with $\delta^{18}O_w = -18.8$ and 99.0‰, especially at temperatures above 15 °C. However, the $\delta^{18}O_p$ values approach, but still do not reach, values expected for equilibrium exchange, even after periods of 30 to 60 days. In some experiments at 15 and 25 °C, only 23–58% of dissolved P_i had equilibrated with the water before these reactions were stopped, or before the bacteria ceased to catalyze the exchange for some other reason (e.g., depletion of a nutrient or cofactor).

In earlier series of experiments carried out in 10 m*M* P_i growth medium with $\delta^{18}O_w = 12.6$‰, it appears that complete equilibration of P_i with water and turnover of the entire dissolved P_i pool took place (Blake et al. 1997; and Table 2). This series of experiments required the largest shift from initial $\delta^{18}O_p$ values to reach equilibrium. Since it is assumed that all P_i-water oxygen isotope exchange occurs intracellularly under these growth conditions, these results, as well as the 5 m*M* P_i experiment in 99.0‰ water, indicate a high flux of P_i through the relatively small intracellular dissolved P_i pool of bacterial cells.

$\delta^{18}O_p$ values slightly more positive than expected were observed for some experiments in 5 m*M* P_i (e.g., 15 and 35 °C, and −8.2‰ water; Table 2). The final $\delta^{18}O$ values of dissolved P_i from 10 m*M* P_i experiments carried out in −6.0 ‰ and −17.7‰ water also were more positive than the expected equilibrium values. For the −6.0‰ experiment, this $\delta^{18}O_p$ value (18.6‰) was also ~7‰ more positive than the starting $\delta^{18}O$ value of dissolved P_i (11.6‰). These positive $\delta^{18}O_p$ values may reflect incorporation of heavier oxygen from a different source, or possibly a kinetic fractionation during uptake or utilization of dissolved P_i by bacteria. As noted above, the process of P_i uptake via transport systems in the cytoplasmic membrane does not require breaking P-O bonds but may involve fractionation of phosphate oxygen by diffusive processes. The possible contribution of such kinetic effects during microbial uptake of P_i remains to be tested, and therefore, cannot be ruled out completely. However, the small and constant size of the bacterial intracellular P_i

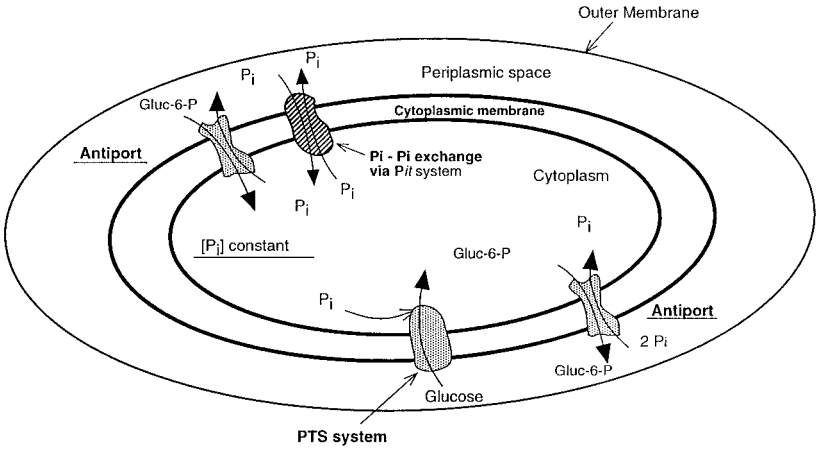

FIGURE 5. Mechanisms of intracellular/extracellular exchange of phosphate via the hexose 6-phosphate:P_i anion antiport system and the P*it* system (P_i:P_i exchange). The sugar phosphotransferase (PTS) system is also shown. Note mechanisms for circulation of phosphate between intracellular and extracellular compartments. Also note that glucose-1-phosphate is not a substrate for the hexose 6-phosphate:P_i antiport system. (Adapted from Ambudkar and Maloney 1984).

pool seems to argue against a kinetic effect to explain the observed shifts of $\delta^{18}O_p$ values. Removal of such a small amount of P_i from the extracellular P_i pool and constant circulation of P_i out of the cell to maintain constant intracellular P_i concentrations, would not allow accumulation of a large enough purely residual (heavy) component of the extracellular P_i pool to make a significant impact on $\delta^{18}O_p$ values of this pool. P_i that has been taken up by the cell, exchanged with water, and then released back into the medium should reflect between zero and 100% exchange with water and therefore, the extracellular P_i pool should have a $\delta^{18}O_p$ value somewhere between the starting value of dissolved P_i and the equilibrium value. Concentrations of dissolved P_i in growth media at the end of the experiments were practically unchanged from the starting values of 5 and 10 m*M* (lower final P_i concentrations in 10 m*M* P_i experiments due to dilution effects; see Blake et al. 1997, Table 1) suggesting that only a small amount of P_i was incorporated into cellular biomass. The total P content of the cells, including P_{org} in cellular biomass, would account for <0.3% of the extracellular P_i pool. Even if some portion of dissolved P_i in the medium were released from the degradation of cellular P_{org} compounds (e.g., DNA, RNA, phospholipids), for example, following the death and lysis of cells, this P_i should have been equilibrated with the water during the intracellular biosynthetic reactions that formed these compounds, and thus, also should not reflect kinetic fractionations. More experimental data are needed to evaluate patterns of isotopic fractionation during bacterial metabolism of phosphate and to establish the presence/absence of kinetic effects during these important processes.

Due to incomplete and different extents of P_i turnover in individual experiments between 5.7 and 30 °C with 5 m*M* P_i, it is difficult to interpret the temperature dependence of phosphate-water oxygen isotope fractionations. Results of these experiments do, however, demonstrate the potential of microbial metabolic processes to make a significant impact on oxygen isotope compositions of the extracellular dissolved P_i pool, even at the relatively high concentrations of P_i used in these experiments. These concentrations of P_i were the lowest possible based on the constraints of current analytical and extraction procedures, but are still much higher than concentrations typical of natural systems (<<100 μM). Thus, similar processes acting in natural systems may be expected to have an even greater impact on $\delta^{18}O_p$ values of dissolved inorganic phosphate, and thus, on the $\delta^{18}O_p$ values of authigenic apatite.

Mechanisms for dissolved P_i turnover and P_i-water oxygen isotope exchange

The patterns of P_i turnover and oxygen isotope exchange observed in these experiments may be compared with proposed models of microbial phosphate utilization for the specific nutrient conditions used here. Following the initial extracellular release of P_i from glucose-1-phosphate, this growth medium was essentially the same as the P_i growth media consisting of glucose + free P_i. The concentrations of dissolved P_i in the P_i media experiments did not decrease appreciably by the end of the experiments yet $\delta^{18}O_p$ values indicate, in several cases, that much or all of the dissolved P_i pool had been turned over and exchanged with water (Tables 1 and 2). Both of these observations are consistent with circulation (or cycling) of dissolved P_i through the intracellular P_i pool of bacterial cells. Such cycling of P_i between intracellular and extracellular compartments is also consistent with proposed models for bacterial growth on the specific medium used in these experiments, a minimal salts glucose + P_i medium (Ambudkar and Maloney 1984; Maloney 1992).

Glucose, which was used as the source of C in these experiments, is not taken up intact by bacterial cells. When grown on glucose as a source of C, many bacteria utilize a group of enzymes called the ''phosphotransferase system'' (PTS), which facilitates the transport of glucose across the cytoplasmic membrane (Fig. 5; Postma 1987). This process involves the phosphorylation and transformation of glucose into glucose-6-phosphate. The P_i used in the phosphorylation of glucose catalyzed by PTS is provided by intracellular sources and, thus, the utilization of glucose as a source of C can lead to depletion of in-

tracellular P_i reserves (Ambudkar and Maloney 1984). It has been proposed that bacteria can replenish the intracellular P_i pool by pumping extracellular P_i into the cytoplasm through membrane-bound proteins called anion antiporters (Fig. 5; Ambudkar and Maloney 1984). Charge balance must be maintained across the antiporters during the transport process to prevent creation of a membrane potential. Thus, as negatively charged P_i is pumped into the cell, an anion of equivalent charge is simultaneously pumped out of the cell. The number of P_i molecules pumped in or out through the antiporter will depend on the amount of charge needed to match the valence of the specific ion being exchanged for P_i (e.g., sugar-phosphate). Because the cell also needs to maintain an overall balance of glucose intake and glucose-6-phosphate metabolism, as well as intracellular P_i levels, this uptake of extracellular P_i is balanced by the pumping of glucose-6-phosphate out of the cell (Fig. 5). This mechanism prevents overaccumulation of intracellular sugar-phosphate when the cell encounters a large pool of glucose, a potentially lethal condition for the cell (Ambudkar and Maloney 1984). As free glucose is depleted from the medium, the cell can then make use of the extracellular glucose-6-phosphate, which is also taken up by an antiporter in exchange for P_i. Exchange of P_i between internal and external P_i pools is also known to occur via the P*it* system for P_i transport (Figs. 1 and 5), which operates under conditions of relatively high external P_i concentrations (Rosenberg et al. 1982).

Thus, conditions are created for the constant cycling or circulation of P_i between intracellular pools—where it is exchanged isotopically with water by enzyme-catalyzed hydrolysis and phosphorylation/dephosphorylation reactions—and the extracellular dissolved P_i pool. The important point to note here is that the cells are not simply utilizing P_i to meet nutritional requirements for P, but rather, to facilitate the transport of glucose to supply the cell with C, which is needed in much higher concentration than P and therefore promotes the recycling of P_i. The very large shifts in $\delta^{18}O_p$ of dissolved P_i observed in many of the experiments with P_i and glucose-1-phosphate media are consistent with this view of the intracellular P_i pool of bacterial cells as a small reservoir with a very high flux of P_i. The much higher concentrations of dissolved P_i generated in the experiments with RNA (90–100 m*M*), and rapid precipitation of this P_i as apatite apparently did not allow further metabolism of the partially exchanged P_i derived from the initial enzymatic hydrolysis of RNA and further exchange and equilibration of this P_i with water via bacterially mediated reactions.

The implication of these processes and the results of our experiments for natural systems where P_i concentrations are much lower, is greatly enhanced recycling of P_i that should, in turn, promote complete exchange and equilibration of oxygen isotopes between dissolved P_i and water under closed system conditions. These results also demonstrate the potential for alteration of $\delta^{18}O_p$ values of mineral phosphates via diagenetic processes involving authigenic precipitation or recrystallization of sedimentary or biogenic apatite in the presence of bacteria. This modification could occur during burial in organic-rich sediments or in the vicinity of a decaying carcass where high concentrations of organic C, P_i, and organophosphorus compounds may be encountered.

Textural features of bacterially synthesized apatites

Interpretations of a bacterial origin of both recent (Rao and Nair 1988; O'Brien et al. 1981; Trichet and Fikri 1997) and ancient (Prevot and Lucas 1986; Soudry and Southgate 1989; Lamboy 1990; Nathan et al. 1990; Bertrand-Sarfati et al. 1997) phosphatic deposits are based almost exclusively on the textural and morphologic features of apatite comprising these deposits. Researchers have commonly interpreted spherical (coccoid), ovoid, or globose occurrences of apatite as the mineralized remains of bacteria. Supporting evidence for interpretating such morphological features as having a microbial origin has been provided by laboratory experiments in which similar structures were produced as a result of microbially mediated precipitation of apatite (Prevot and Lucas 1986; Hirschler et al. 1990). Unique crystal habits have also been observed for bacterially induced precipitates of calcium carbonate in laboratory experiments and in natural samples (e.g., Buczynski and Chafetz 1991).

The apatite minerals synthesized in experiments reported here and previously (Blake et al. 1997) were examined by SEM and several interesting textural features were observed (Figs. 6 and 7). The $CaCO_3$ (aragonite) substrates used in the apatite synthesis experiments included *Halimeda* (green algae), cuttle bone, and coral, which had high initial surface areas to promote reaction (Figs. 6a and 6b). The microbial apatites comprised small, sub-micrometer sized-spherical structures (Figs. 6c, 6e, and 6g) encrusting the remains of calcium carbonate substrates that maintained their original morphology although replaced completely by apatite. Prévôt and Lucas (1986) and Hirschler et al. (1990, 1992) observed similar pseudomorphic replacement of carbonate precursors by microbially produced apatites synthesized in laboratory experiments. Spherical structures resembling those observed by these authors in natural phosphorite specimens have been interpreted to be bacterial in origin (e.g., Prévôt and Lucas 1986; Lamboy 1990).

In Figures 6c–6h, fluorapatites precipitated in experiments with bacteria (microbial apatites; on the left) are compared with fluorapatites precipitated in inorganic control experiments without bacteria present (inorganic apatites; on the right). Comparison of morphological features of microbial and inorganic apatites reveal striking similarities. Figures 6c and 6d show similar encrusting, micrometer and sub-micrometer-sized spherical structures in both microbial and inorganic apatites. Upon closer examination of these structures, some distinguishing features can be observed. First, the spherical grains in the microbial apatites are in the appropriate size range for bacteria (~0.5–3 μm) and are more uniform individual

''free'' spheres (Figs. 6c, 6e, and 6g). By contrast, the spherical structures in inorganic apatites have more varied sizes and shapes comprising clumped aggregates with a more botryoidal texture (Figs. 6d, 6f, 6h, and 7g), and typically have much larger sizes of <1 μm to ~ 10 μm (Figs. 6d and 6f). Such dimensions are quite large for bacteria, most of which have diameters of <1–3 μm. Algal and cyanobacterial cells, however, are known to have similar spherical shapes and larger dimensions of up to ~ 50 μm (Schopf 1977). These observations confirm the results of Hirschler et al. (1992), who also observed similar morphologic features in microbially synthesized apatites and apatites produced under sterile conditions in inorganic phosphate solutions.

When hydroxyapatite was precipitated instead of fluorapatite, by omitting NaF from the reaction medium, quite different textures were produced in both microbial apatites (Fig. 6i) and inorganic apatites (Fig. 6j). This observation suggests that the formation of smooth spheroidal structures is somehow unique to fluorapatite, which probably is related to its higher degree of crystallinity.

Spheroidal structures were also produced as what appear to be dissolution remnants in apatites precipitated in experiments with glucose-1-phosphate and *K. aerogenes* (Figs. 7a–7f). Following an initial rise, concentrations of P_i decreased to 4–5.7 m*M* (at pH 8) at the end of experiments, which may have created conditions of undersaturation with respect to apatite (possibly locally near bacterial-mineral interfaces). The surfaces of mineral specimens shown in Figures 7a–7e are covered with pits or molds of the appropriate size and shape for bacteria. Figure 7b (arrow) shows what appears to be bacterial cells positioned in-place within these molds. Davis and Briggs (1995) observed similar honeycomb-like textures in what was identified as fossilized bacterial glycocalyx. Glycocalyx is an exocellular polysaccharide polymer secreted by some bacteria and used to attach to solid substrates, trap nutrients, and act as a protective cover for bacterial colonies (Davis and Briggs 1995).

Hirschler et al. (1992) performed detailed SEM and TEM analyses of the relations between bacterial cells and synthetic apatites to determine the site of apatite precipitation and the possible role of bacteria as nucleation sites for this mineralization. In their experiments, the strains *Escherichia coli* NCIB 8545 and *Providencia rettgeri* did not serve as nucleation sites for precipitation of spheroidal apatite structures nor were the cells mineralized as a result of apatite precipitation. The textures observed here also argue against the bacteria serving as nucleation sites for precipitation of the spheroidal structures, because the molds are distributed throughout the spheres as opposed to being located at their cores (Figs. 7b and 7c). Bacteria still may have played a role in nucleating apatite precipitation. Note that the pits and molds have smooth surfaces and are of rather uniform and undistorted size and shape (Figs. 7c–7e). Furthermore, in some cases, it appears that the crystals grew around or outward perpendicularly from the edges of these molds (Figs. 7d and 7e). Kohn et al. (1998, this volume) observed 0.5–1 μm circular structures on the interiors of framboidal pyrite grains and suggested a possible role of bacteria as nucleation sites for precipitation of these Fe-sulfide minerals on the basis of chemical and isotopic evidence as well as morphology.

It is proposed here that the bacteria were first mineralized and subsequently engulfed by a matrix of apatite. As the concentration of P_i in solution decreased, the apatite began to dissolve and the mineralized bacteria were ''weathered out'' leaving the observed molds and pits. This scenario is also supported by the observation of what appear to be bacterial cells that have been replaced by apatite (Figs. 7b and 7f). Phosphatized bacterial cells have been reported in recent and ancient phosphorite deposits (e.g., O'Brien et al. 1981; Rao and Nair 1988; Bertrand-Sarfati et al. 1997). The observed textures may be unique to the laboratory conditions employed in the conduct of these experiments. Nonetheless, these studies demonstrate that spheroidal textures may be produced as a result of dissolution processes as well as in the precipitation of fluorapatite. The close association between bacterial cells and apatite minerals observed here and in prior studies may also have important implications for the formation of other important secondary phosphate minerals such as Al, Fe and rare-earth phosphates (e.g., Banfield and Eggleton 1989).

Long-term experiments were also carried out to investigate the effects of aging on apatite crystallinity. Inorganic fluorapatite formed at 25 °C (Fig. 7g) and aged for over two years (Fig. 7h) shows various recrystallization textures as well as radial fibrous crystals and ''dumbbell'' structures. Overall, the crystal aggregates are uniformly larger. Microbial apatites also show evidence of recrystallization to much larger, euhedral, radial fibrous crystals (Figs. 7i and 7j) with increasing age. Taken together, the textural features observed in laboratory synthesized apatite minerals demonstrate that interpretation of sedimentary structures as microbial in origin solely on the basis of morphological and textural features may be misleading.

Summary and conclusions

Bacterial metabolic processes can significantly alter $\delta^{18}O_p$ values of dissolved inorganic phosphate in laboratory culture experiments, even at high dissolved P_i concentrations. Oxygen isotope compositions of dissolved P_i measured in bacterial growth experiments support models for microbial utilization of P_i under specific nutrient conditions and indicate significant recycling of the dissolved P_i pool. In natural environments, where concentrations of dissolved P_i are typically low, these processes should be magnified. This condition, in turn, should lead to complete exchange and equilibration of oxygen isotopes between P_i and environmental water under closed-system conditions. $\delta^{18}O_p$ values of P_i removed from the dissolved P_i pool prior to complete turnover, for example, by pre-

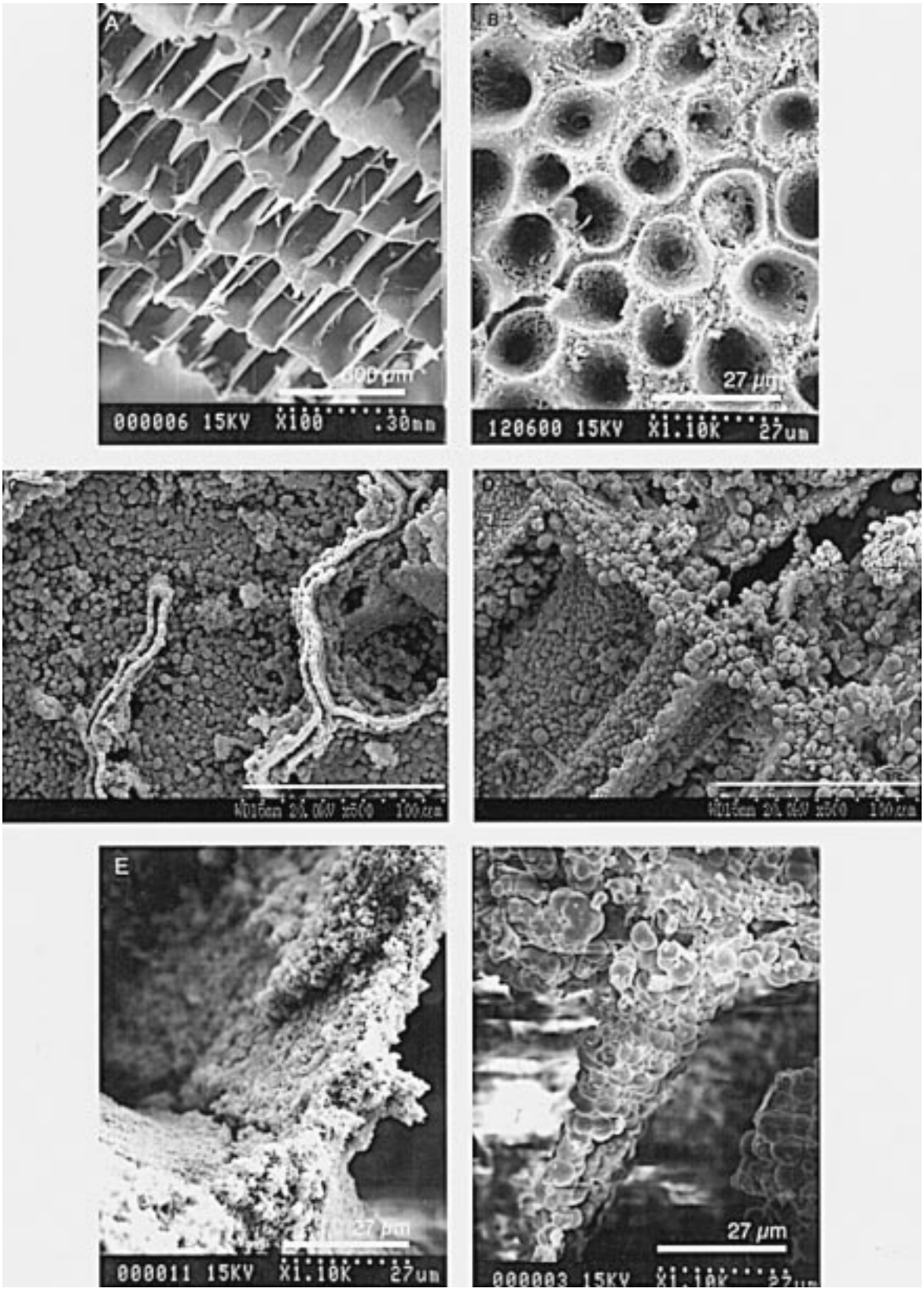
A
000006 15KV X100 .30mm
B
27 µm
120600 15KV X1.10K 27um
C
D
E
000011 15KV X1.10K 27um
27 µm
000003 15KV X1.10K 27um

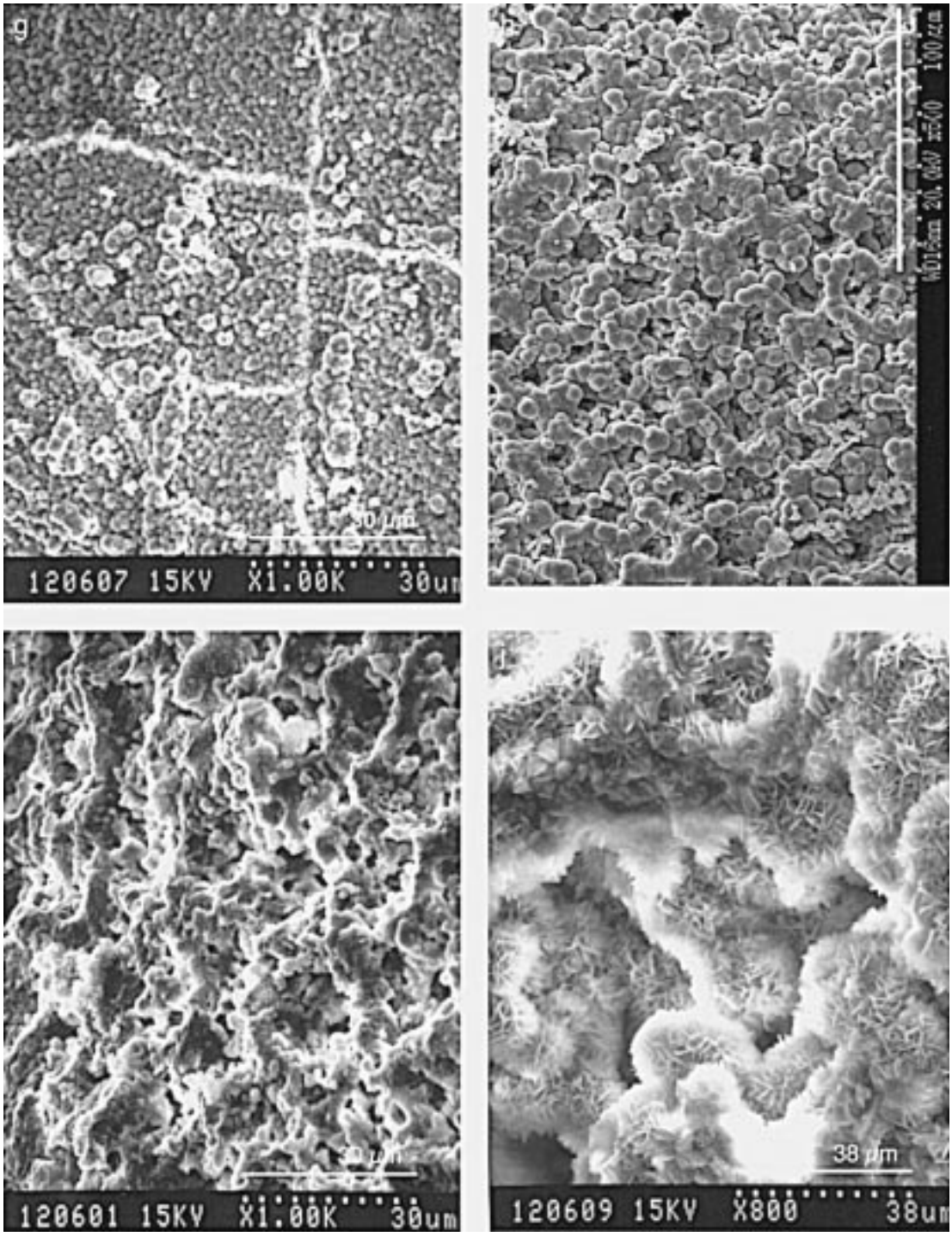

FIGURE 6. SEM images of aragonitic substrates and synthetic apatites. Fluorapatites formed in the presence of bacteria (microbial apatites: c, e, and g on left). Inorganic fluorapatites formed abiotically without bacteria (inorganic apatites: d, f, and h on right). (**a**) Cuttle bone and (**b**) *Halimeda* aragonitic substrates with high surface areas to promote reaction. (**c**) Microbial apatite on cuttle bone substrate. (**d**) Inorganic apatite on cuttle bone substrate. (**e**) Microbial apatite on cuttle bone. Note submicrometer-sized spherical apatite structures of very uniform size. (**f**) Inorganic apatite on cuttle bone substrate. Note large, non-uniform sized spheres with botryoidal texture. (**g**) Microbial apatite on coral substrate. Note uniform size and individual ''free'' spheres compared with inorganic precipitate (**h**). (**i**) Microbial hydroxyapatite on *Halimeda* substrate showing no clear structure or spheroidal features. (**j**) Inorganic hydroxyapatite showing characteristic bladed crystal aggregates.

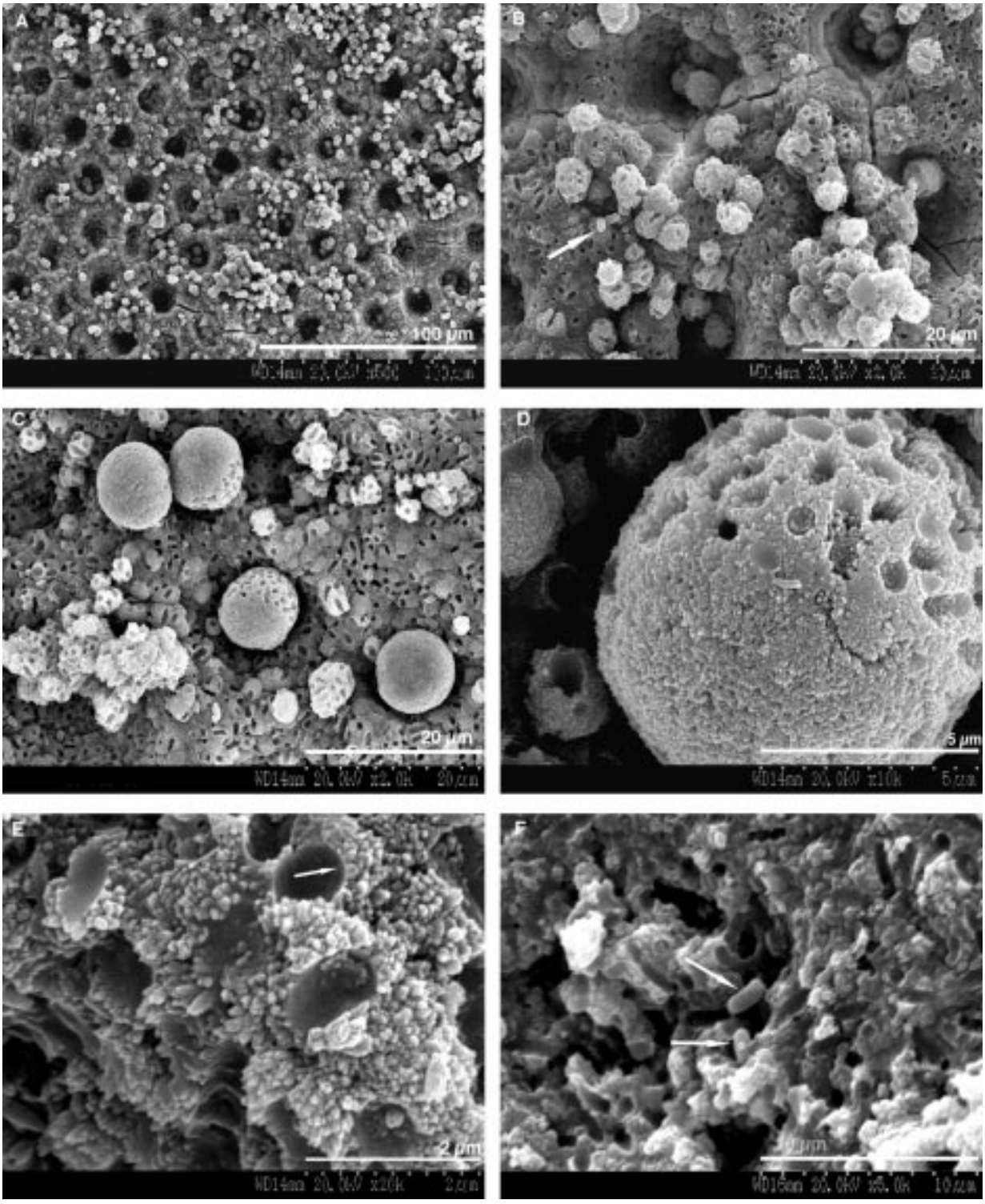

Figure 7. SEM images showing dissolution, nucleation and recrystallization textures in microbial apatites. (**a**)–(**f**) Apatites from glucose-1-phosphate growth experiments with *K. aerogenes* showing apparent dissolution textures. (**a**) Low magnification image of apatite on *Halimeda* substrate showing individual and aggregate spherical structures of uniform size. (**b**) Close-up of **a** revealing surface covered with pits/molds of the approximate size and shape of bacterial cells. Arrow shows possible bacterial cells in-situ. (**c**) Larger spherical structures showing strong evidence of preferential dissolution on one side. Note how smaller spherical structures appear to be weathering out of the back ground substrate. (**d**) Close-up of spherical structure in center of **c** showing apparent growth of crystals around edges of molds suggesting that molds contained relatively hardened structures, possibly apatized bacterial cells.

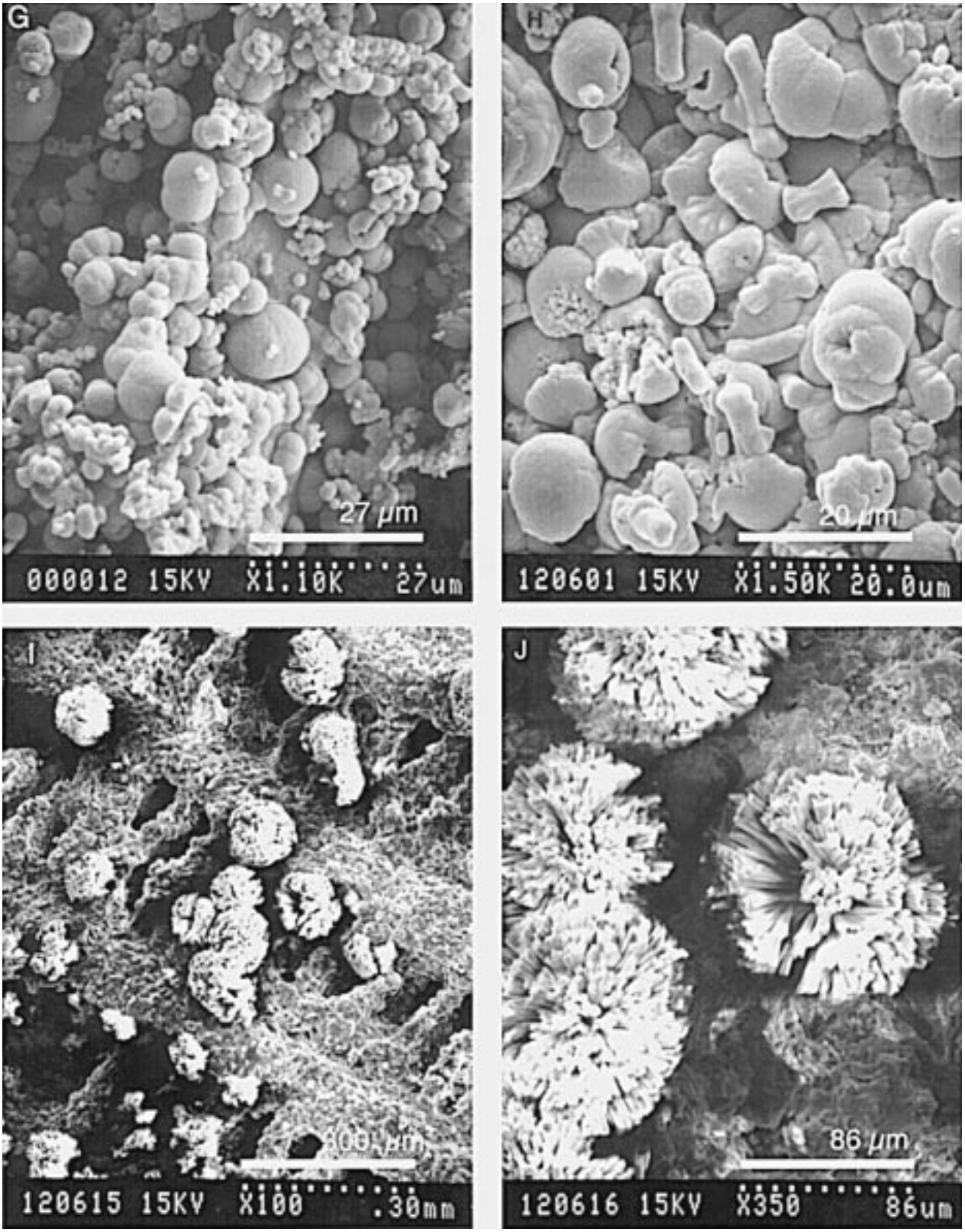

FIGURE 7. Continued. (**e**) High magnification image of molds showing smooth interior surfaces and growth of crystals around or perpendicularly outward from (arrow) edges of mold suggesting nucleation of crystal on object formerly within the mold. (**f**) Structures that appear to be bacterial cells that have been replaced by apatite (arrows). (**g**) Fresh and (**h–j**) Aged inorganic (**g, h**) and microbial (**i, j**) apatites showing recrystallization to larger, more uniform and euhedral crystal habits.

cipitation of authigenic apatite will reflect only partial exchange with water.

Importantly, not all of the dissolved P_i released from organic matter by extracellular bacterial enzymes may be taken up immediately by the cells and further metabolized and exchanged with water. Instead, some of this partially exchanged extracellular P_i may become involved in other processes such as precipitation of authigenic phosphate minerals.

Results presented here and in previous experimental studies on the role of bacteria in apatite synthesis (Hirschler et al. 1992) demonstrate that spherical and coccoid structures can be produced readily during inorganic or microbially mediated precipitation of fluorapatite and, therefore, are not diagnostic of microbial mediation in apatite precipitation, but may be unique to fluorapatite precipitation. Thus, caution should be exercised when interpreting similar structures in natural specimens. Preferably, some criteria in addition to morphology, such as chemical composition (e.g., distinctive biomolecules) or other chemical evidence (e.g., Banfield and Eggleton 1989; Kohn et al., this volume) should be used when interpreting such morphological features.

Acknowledgments

This work was supported by NSF grants EAR-9406067 to J.R.O. and EAR-9628196 to the University of Michigan Electron Microbeam Analysis Laboratory (EMAL), and by a University of Michigan Rackham Graduate School Research Partnership Award to R.E.B. and G.A.G. T.J. Huston, J.R. Hansen, M.A. Cousins (Purdue University) and S.J. Birnbaum (University of Texas, San Antonio) are thanked for analytical support and consultation. We especially thank L.M. Walter for the use of facilities and equipment at the University of Michigan Experimental and Analytical Geochemistry Laboratory (EAGL). M.J. Kohn is thanked for a very thorough and insightful review that greatly improved this manuscript. We also thank J. Banfield and an anonymous reviewer for their helpful comments and suggestions.

References cited

Ambudkar, S.V. and Maloney, P.C. (1984) Characterization of phosphate: hexose 6-phosphate antiport in membrane vesicles of Streptococcus lactis. Journal of Biological Chemistry, 259, 12576–12585.

Ammerman, J.W. (1991) Role of ecto-phosphohydrolases in phosphorus regeneration in estuarine and coastal ecosystems. In R. Chróst, Ed., Microbial Enzymes in Aquatic Environments, p. 165–185. Springer-Verlag, New York.

Ayliffe, L.K. and Chivas, A.R. (1990) Oxygen isotope composition of the bone phosphate of Australian kangaroos: Potential as a paleoenvironmental indicator. Geochimica et Cosmochimica Acta, 54, 2603–2609.

Banfield, J.F. and Eggleton, R.A. (1989) Apatite replacement and rare earth element mobilization, fractionation, and fixation during weathering. Clays and Clay Minerals, 37, 113–127.

Barrick, R.E. and Showers, W.J. (1994) Thermophysiology of Tyrannosaurus rex: Evidence from oxygen isotopes. Science, 265, 222–227.

Bennett, P.C., Hiebert, F.K., and Choi, W.J. (1996) Microbial colonization and weathering of silicates in a petroleum-contaminated groundwater: Chemical Geolology, 132, 45–53.

Bertrand-Sarfati, J., Flicouteaux, R., Moussine-Pouchkine, A., and Ahmed, A.A.K. (1997) Lower Cambrian apatitic stromatolites and phospharenites related to the glacio-eustatic cratonic rebound (Sahara, Algeria). Journal of Sedimentary Research, 67, 957–974.

Blake, R.E., O'Neil, J.R., and Garcia, G.A. (1997) Oxygen isotope systematics of microbially mediated reactions of phosphate: I. Degradation of organophosphorus compounds. Geochimica et Cosmochimica Acta, 262, 4411–4422.

Brown, D.A., Sherriff, B.L., and Sawicki, J.A. (1997) Microbial transformation of magnetite to hematite. Geochimica et Cosmochimica Acta, 61, 3341–3348.

Bruice, T.C., Blaskó, A., Arasasingham, R.D., and Kim, J-S. (1995) Participation of two carboxyl groups in phosphodiester hydrolysis: 2. A kinetic, isotopic, and ^{31}P NMR study of the hydrolysis of a phosphodiester with carboxyl groups fixed in an attack conformation. Journal of the American Chemical Society, 117, 12070–12077.

Buczynski, C. and Chafetz, H.S. (1991) Habit of bacterially induced precipitates of calcium carbonate and the influence of medium viscosity on mineralogy. Journal of Sedimentary Petrology, 61, 226–233.

Chróst, R.J. (1991) Environmental control of the synthesis and activity of aquatic microbial ectoenzymes. In R. Chróst, Ed., Microbial Enzymes in Aquatic Environments, p. 29–59. Springer-Verlag, New York.

Cohn, M. and Urey, H.C. (1938) Oxygen isotope exchange reactions of organic compounds and water. Journal of the American Chemical Society, 60, 679–682.

D'Angela, D. and Longinelli, A. (1993) Oxygen isotopic composition of fossil mammal bones of Holocene age: Paleoclimatological considerations. Chemical Geology, 103, 171–179.

Davis, P.G. and Briggs, D.E.G. (1995) Fossilization of feathers. Geology, 23, 783–786.

Folk, R.L. (1993) SEM imaging of bacteria and nannaobacteria in carbonate sediments and rocks. Journal of Sedimentary Petrology, 63, 990–999.

Folk, R.L. and Lynch, F.L. (1997) The possible role of nannobacteria (dwarf bacteria) in clay-mineral diagenesis and the importance of careful sample preparation in high-magnification SEM study. Journal of Sedimentary Research, 67, 583–589.

Fricke, H.C., Clyde, W.C., O'Neil, J.R., and Gingerich, P.D. (1996) Continental paloeclimate across the Paleocene/Eocene boundary as inferred from variations in $\delta^{18}O$ (PO_4) of mammalian tooth enamel and fish scales. Geological Society of America Abstracts with Programs, 28.

Goldstein, A.H. (1994) Involvement of the quinoprotein glucose dehydrogenase in the solubilization of exogenous mineral phosphates by gram-negative bacteria. In A. Torriani-Gorini et al., Ed., Phosphate in Microorganisms: Cellular and Molecular Biology, p. 197–203. American Society for Microbiology.

Grantham, M.C. and Dove, P.M. (1997) Microbially catalyzed dissolution of iron and aluminum oxyhydroxide mineral surface coatings. Geochimica et Cosmochimica Acta, 61, 4467–4477.

Gruau, G. (1997) Oxygen isotope analyses as a tool to detect the origin and fate of phosphates in eutrophic water systems. Geological Society of America Annual Meeting, Salt Lake City, Utah. Abstracts with Program, 29.

Hirschler, A., Lucas, J., and Hubert, J. (1990) Bacterial involvement in apatite genesis: FEMS Microbiology Ecology, 73, 211–220.

———(1992) Apatite genesis: A biologically induced or biologically controlled mineral formation process. Geomicrobiology Journal, 7, 47–57.

Ingall, E.D., Schroeder, P.A., and Berner, R.A. (1990) The nature of organic phosphorus in marine sediments: New insights from ^{31}P NMR. Geochimica et Cosmochimica Acta, 54, 2617–2620.

Jones, B. (1995) Processes associated with microbial biofilms in the twilight zone of caves: Examples from the Cayman Islands. Journal of Sedimentary Research, A65, 552–560.

Kadner, R.J., Island, M.D., Merkel, T.J., and Webber, C.A. (1994) Transmembrane control of the Uhp sugar-phosphate transport system: The sensation of Glu6P. In A. Torriani-Gorini et al., Ed., Phosphate in Microorganisms: Cellular and Molecular Biology, p. 78–84. American Society for Microbiology.

Kohn, M.J., Schoeninger, M.J., and Valley, J.W. (1996) Herbivore tooth oxygen isotope compositions: Effects of diet and physiology. Geochimica et Cosmochimica Acta, 60, 3889–3896.

Kohn, M.J., Riciputi, L.R., Stakes, D., and Orange, D.L. (1998) Sulfur isotope variability in biogenic pyrite: Reflections of heterogeneous bacterial colonization? American Mineralogist, 83, 1452–1466.

Kolodny, Y., Luz, B., and Navon, O. (1983) Oxygen isotope variations

in phosphate of biogenic apatites, I. Fish bone apatite—rechecking the rules of the game. Earth and Planetary Science Letters, 64, 398–404.

Konhauser, K.D., Fyfe, W.S., Schultze-Lam, S., Ferris, F.G., and Beveridge, T.J. (1994) Iron phosphate precipitation by epilithic microbial biofilms in Arctic Canada. Canadian Journal of Earth Sciences, 31, 1320–1324.

Koroleff, F. (1983) Determination of phosphorus: In K. Grasshoff et al., Ed., Methods of Seawater Analysis, 2nd ed., p. 125–187. Verlag Chemie.

Kroopnick, P.M. and Craig, H. (1972) Atmospheric oxygen: isotopic composition and solubility fractionation. Science, 175, 54–55.

Kulaev, I. (1994) Introduction: Polyphosphates and phosphate reserves. In A. Torriani-Gorini et al., Ed., Phosphate in Microorganisms: Cellular and Molecular Biology, p. 195–196. American Society for Microbiology, Washington, D.C.

Lamboy, M. (1990) Microbial mediation in phosphatogenesis: new data from the Cretaceous phosphatic chalks of northern France. In A.J.G. Notholt and I. Jarvis, Eds., Phosphorite Development and Research, 52, 157–167. Geological Society Special Publication,

Lécuyer, C., Grandjean, P., and Emig, C.C. (1996) Determination of oxygen isotope fractionation between water and phosphate from living lingulids: potential application to paleoenvironmental studies: Palaeogeography, Palaeoclimatology, Palaeoecology, 126, 101–108.

Longinelli, A. (1993) Oxygen isotopes in mammal bone phosphate: A new tool for paleohydrological and paleoclimatological research? Geochimica et Cosmochimica Acta, 48, 385–390.

Longinelli, A. and Nuti, S. (1973) Revised phosphate-water isotopic temperature scale. Earth and Planetary Science Letters, 19, 373–376.

Lovely, D.R., Stoltz, J.F., Nord, G.L. Jr., and Phillips, E.J.P. (1987) Anaerobic production of magnetite by a dissimilatory iron-reducing microorganism. Nature, 330, 252–254.

Lucas, J. and Prévôt, L., (1984) Synthèse de l'apatite par voie bacterienne á partir de matière organique phosphatée et de divers carbonates de calcium dans des eaux douce et marine naturelles. Chemical Geology, 42, 101–118.

Luz, B. and Kolodny, Y. (1985) Oxygen isotope variations in phosphate of biogenic apatites: IV. Mammal teeth and bones. Earth and Planetary Science Letters, 75, 29–36.

Maloney, P.C. (1992) The molecular and cell biology of anion transport by bacteria. BioEssays, 14, 757–762.

Mandernack, K.W., Fogel, M.L., Tebo, B.M., and Usui, A. (1995) Oxygen isotope analyses of chemically and microbially produced manganese oxides and manganates. Geochimica et Cosmochimica Acta, 59, 4409–4425.

Markel, D., Kolodny, Y., Luz, B., and Nishri, A. (1994) Phosphorus cycling and phosphorus sources in Lake Kinneret: Tracing by oxygen isotopes in phosphate. Israeli Journal of Earth Science, 43, 165–178.

Nathan, Y., Soudry, D., and Avigour, A. (1990) Geological significance of carbonate substitution in apatites: Israeli phosphorites as an example. In A.J.G. Notholt and I. Jarvis, Eds., Phosphorite Development and Research. Geological Society Special Publication, 52, 179–191.

Neidhardt, F.C. (1987) Chemical composition of Escherichia coli. In F.C. Neidhardt, Ed., Escherichia coli and Salmonella typhimurium, Cellular and Molecular Biology, p. 3–6. American Society for Microbiology, Washington, D.C.

O'Brien, G.W., Harris, J.R., Milnes, A.R., and Veeh, H.H. (1981) Bacterial origin of East Australian continental margin phosphorites. Nature, 294, 442–444.

Oehler, J.H. (1975) Origin and distribution of silica lepispheres in porcelanite from the Monterey Formation of California. Journal of Sedimentary Petrolology, 45, 252–257.

O'Neil, J.R., Roe, L.J., Reinhard, E., and Blake, R.E. (1994) A rapid and precise method of oxygen isotope analysis of biogenic phosphate. Israeli Journal of Earth Sciences, 43, 203–212

Paul, E.A. and Clark, F.E. (1989) Soil Microbiology and Biochemistry. Academic Press, 227–229.

Paytan, A. (1989) Oxygen isotope variations of phosphate in aquatic systems. Master's thesis, Hebrew University, Jerusalem.

Postma, P.W. (1987) Phosphotransferase system for glucose and other sugars. In F.C. Neidhardt et al., Ed., Escherichia coli and Salmonella typhimurium, Cellular and Molecular Biology, vol. 1, Chap. 11, 127–141. American Society for Microbiology, Washington, D.C.

Prévôt, L. and Lucas, J. (1986) Microstructure of apatite-replacing carbonate in synthesized and natural samples. Journal of Sedimentary Petrology, 56, 153–159.

Rao, V.P and Nair, R.R. (1988) Microbial origin of the phosphorites of the western continental shelf of India. Marine Geolology, 84, 105–110.

Rao, N.N., Kar, A., Roberts, M.F., Yasphire, J., and Torriani-Gorini, A. (1994) Phosphate, phosphorylated metabolites, and the Pho regulon of Escherichia coli. In A. Torriani-Gorini et al., Ed., Phosphate in Microorganisms: Cellular and Molecular Biology, 195–196. American Society for Microbiology, Washington, D.C.

Rosenberg, H. Lesley, M.R. Jacomb, P.A., and Chegwidden, K. (1982) Phosphate exchange in the Pit transport system in Escherichia coli. Jour. Bacteriology, 149, 123–130.

Schopf, J.W. (1977) Biostratigraphic usefullness of stromatolitic Precambrian microbiotas: A preliminary analysis. Precambrian Research, 5, 143–173.

Soudry, D. (1987) Ultra-fine structures and genesis of the Campanian Negev high-grade phosphorites (southern Israel). Sedimentology, 34, 641–660.

Soudry, D. and Southgate, P.N. (1989) Ultrastructure of a Middle Cambrian primary nonpelletal phosphorite and its early transformation into phosphate vadoids: Georgina Basin, Australia. Journal of Sedimentary Petrolology, 59, 53–64.

Trichet, J. and Fikri, A. (1997) Organic matter in the genesis of high-island atoll peloidal phosphorites: the lagoonal link. Journal of Sedimentary Research, 67, 891–897.

Ullman, W.J., Kirchman, D.L., Welch, S.A., and Vandevivere, P. (1996) Laboratory evidence for microbially mediated silicate mineral dissolution in nature: Chemical Geology, 132, 11–17.

Vasconcelos, C. and McKenzie, J. (1997) Microbial mediation of modern dolomite precipitation and diagenesis under anoxic conditions (Lagoa Vermelha, Rio De Janeiro, Brazil). Journal of Sedimentary Research, 67, 378–390.

Manuscript received March 9, 1998
Manuscript accepted August 21, 1998
Paper handled by Jillian F. Banfield